

**UNIVERSITY OF CRAIOVA**  
**FACULTY OF MATHEMATICS AND NATURAL SCIENCE**

**CHIȘ G.-M. ANDREEA CARMEN (căș. ANDREI)**

**Laser processing of thin films with functional properties -  
applications of ferroelectric materials**

– Thesis summary -

PhD Advisor:

**Scientific Researcher I**

**Dr. DINESCU Maria**

Craiova

2014

# Cuprins

<b>Introduction.....</b>	<b>3</b>
<b>Capitolul 1: Materiale feroelectrice.....</b>	<b>5</b>
1.1 The History of Ferroelectrics.....	5
1.2 General properties of Ferroelectrics.....	5
1.3 Applications of the ferroelectric materials.....	7
1.4 Types of ferroelectric materials.....	7
<b>Capitolul 2: Deposition and characterization techniques of ferroelectric thin films.....</b>	<b>7</b>
2.1 Deposition techniques of ferroelectric thin films.....	7
2.2 Utilized deposition techniques – PLD.....	8
2.3 Characterization methods of ferroelectric thin films.....	10
<b>Capitolul 3:Deposition and characterization of thin ferroelectric film with lead PLZT.....</b>	<b>10</b>
3.1 Experimental conditions.....	11
3.2 Results and discussion.....	12
3.3. Conclusions.....	17
<b>Capitolul 4: Depunerea și caracterizarea de filme subțiri feroelectrice fără plumb NBT....</b>	<b>18</b>
4.1 Experimental conditions.....	19
4.2 Results and discussions – comparison between the NBT and NBT-BT6.....	20
4.3 Results and discussion – characterization of NBT-BT6 films.....	22
4.4 Conclusions.....	26
<b>General conclusions.....</b>	<b>27</b>
<b>Scientific articles.....</b>	<b>31</b>
<b>Selective Bibliography.....</b>	<b>32</b>

## Introduction

Modern electronic devices such as personal computers, MP3 players, or mobile phones are objects without which life nowadays is inconceivable. The speed with which these devices miniaturize and modernize has grown exponentially in the last few years, having a strong connection with the development of high performance materials and technologies. In the composition of all of these devices there are sub-ensembles that contain piezoelectric and ferroelectric materials. Another field in which these materials are present is that of sensors. In this context, research regarding obtaining new materials, as well as improving the properties of the already existing ones are intense. Obtaining thin films from ferroelectric materials is given particularly special attention, due to the necessities imposed by the continuous miniaturization of equipment/devices.

Lead zirconate titanate (PZT) is the material most utilized from a commercial point of view due to its ferroelectric and piezoelectric properties, having numerous applications, such as infrared sensors, condensers, RAM memories, MEMS, etc. Its principal disadvantage derives from the fact that it contains lead. Due to considerations linked to the protection of the environment, the European Union has even created the RoHS policy (Restriction of Harmful Substances, 2011/65/EU) regarding the restriction of use for certain dangerous elements in the industry (lead, cadmium, mercury, hexavalent chromium, etc.). The initial deadline present in these policies is considered solely informative, as materials with similar properties must exist in order to replace the ferroelectric/ piezoelectric systems, based on lead. In consequence, materials with as small a concentration of lead as possible, or even without lead, constitute the main focus of the scientific community. Amongst these, I have chosen lead zirconate titanate doped with lanthanum (PLZT) and sodium and bismuth titanate (NBT) and respectively sodium and bismuth titanate doped with barium titanate (NBT-BT). In the case of PLZT I have pursued the improvement of the optical and dielectric properties of the material, in the form of a thin film, as well as diminishing the toxic effects caused by the use lead titanate and zirconium (PZT) by doping it with lanthanum. For the composites with sodium titanate and bismuth bases (NBT and NBT-BT) I have investigated the influence of experimental conditions, such as the deposition

temperature and the BT content of the target on the crystalline structure, the dielectric properties, and the phase transition temperature of thin films.

This paper is structured in 4 chapters, completed by the introductory chapter and the cumulative bibliography of the work; the end will contain an attachment with the list of the candidate's publications, as well as presentations at specialist conferences, both local and international.

The introductory chapter presents the theme of the thesis and the importance of the field in which the paper is situated, as well as the range of practical applications. Additionally, the motivation for selecting this theme, as well as the structure of the thesis, will be presented.

Chapter 1, entitled *Ferroelectric materials*, will present the class of ferroelectric materials: dipolar dielectric materials, which present a spontaneous electric polarization which can be commuted through the application of an external electric field. The important moments in their development will be described, as well as their principal properties such as the phase transitions, ferroelectric domains, the perovskite type structure etc. Additionally, the properties important for modern technology will be presented. This chapter also describes the most important types of ferroelectric materials, with and without lead.

Chapter 2, entitled *Methods of obtaining and characterizing thin ferroelectric films*, contains information related to the techniques of deposition utilized for obtaining ferroelectric materials in the form of thin films, outlining the method utilized by this thesis, respectively the pulsed laser deposition. This chapter also revises the principal techniques utilized for morphologic and structural characterizations, such as AFM (Atomic Force Microscope), SEM (Scanning Electron Microscope), SE (Spectral Ellipsometry), XRD (X-Ray Diffraction), TEM (Transmission Electron Microscope), as well as electric and ferroelectric characterization methods.

Chapter 3, *The deposition and characterization of thin ferroelectric films with lead – PLZT*, describes the properties of the respective material, as well as the parameters used in obtaining the thin films of lead zirconate titanate doped with lanthanum by PLD. The experimental results obtained regarding the morphology of the surface (AFM and SEM studies) and the crystallinity (X-ray diffraction) are also presented and discussed. The same chapter

contains a description of the optical, electro-optical, as well as dielectric and ferroelectric properties of the films obtained.

Chapter 4, *The deposit and characterization of thin ferroelectric films without lead – NBT and NBT-BT6*, investigates thin ferroelectric films made from sodium titanate and bismuth doped with barium titanate with different concentrations of dopant. The properties of these materials are presented, as well as their area of applicability and the parameters utilized for obtaining them in the form of thin films through pulsed laser deposit. This chapter reports the structural and morphological properties, as well as the dielectric and ferroelectric characteristics of the films obtained.

Each chapter is accompanied by a specialized bibliography, which contains both titles of papers/traditional and fundamental books in the field, as well as publications from very recent dates.

## **Chapter 1: Ferroelectric Materials**

### **1.1 The History of Ferroelectrics**

The ferroelectrics phenomenon was first discovered in 1921 in the Rochelle salt. This salt was first created in the laboratory of the Seignette brothers, in the seventeenth century, to be used for medicinal purposes. The name of ferroelectrics was assigned in analogy with ferromagnetism, which is the property of certain metals and alloys to have a spontaneous magnetic order.

Ferroelectric materials are a class of dielectric dipolar materials that present an electric spontaneous polarization which can be reversed through the application of an external electric field. This unique characteristic is a very interesting research topic, both for fundamental physics as well as mechanic and electric engineering.

### **1.2 General properties of Ferroelectrics**

Ferroelectrics are polar materials, belonging to the family of piezoelectrics, which have at least two equilibrium orientations of the spontaneous polarization vector, in the absence of an

electric field. In the presence of an external electric field, the spontaneous polarization vector can commute between the two equilibrium orientations.

From the point of view of symmetry, all ferroelectric crystals belong to one of the 10 punctual polar groups (pyroelectric crystals). The 10 polar crystallographic groups are part of the family of 20 punctual noncentrosymmetric groups which present the piezoelectric effect, also called punctual piezoelectric groups, resulting that any ferroelectric is pyroelectric and any pyroelectric is piezoelectric.

At the same time, these are also piezoelectric. The piezoelectric effect consists of the appearance of a charge when applying a mechanical tension to the crystal. The charge appears as a result of the modification of the position of atoms under the action of the applied mechanical tension, leading to the modification of the spontaneous polarization. In addition, ferroelectric materials also present pyroelectric properties.

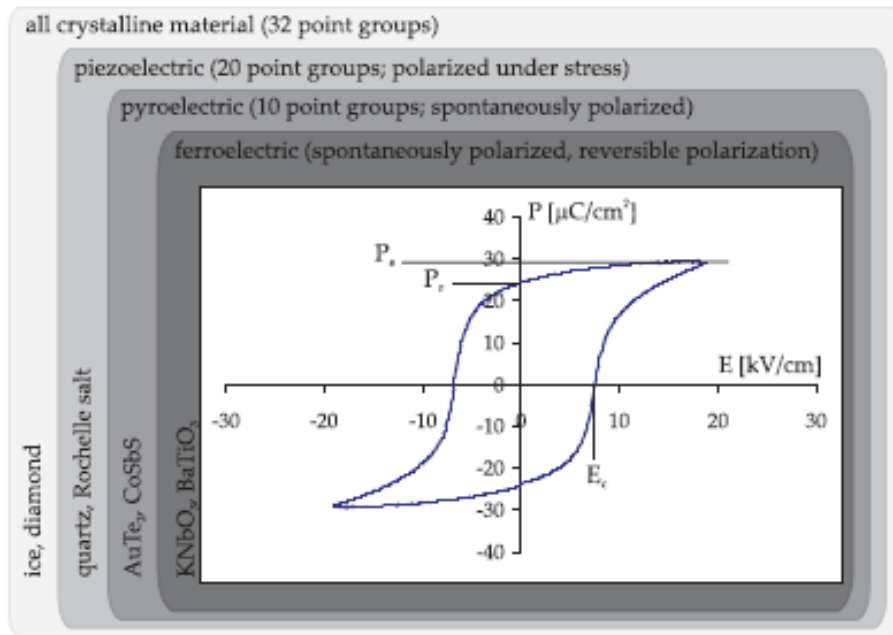


Figure 1. Diagram of the crystallographic groups and sub-groups that define piezoelectricity, pyroelectricity and ferroelectricity. Vertically, there are some examples of materials and each sub-group. Above there is the typical hysteresis curve of a ferroelectric material. [1]

Ferroelectric materials allow a structural phase transition from the ferroelectric state in

low temperatures, to the paraelectric state (or non-ferroelectric), in high temperatures. This thermic movement can destroy the ferroelectric order, and symmetry in the case of the paraelectric state is always higher than that in the case of the ferroelectric phase. The temperature at which the phase transition takes place has the name of Curie point,  $T_c$ .

Most of the ferroelectric materials have a perovskite-type structure, and this structure is ideally cubical, with the formula  $ABO_3$ , the A cations being located at the corner of the cube (mono or bivalent metals), the B cations at the center of the cube, and the  $O_2$  anions situated at the centers of the cube's sides.

### **1.3 Applications of the ferroelectric materials**

Ferroelectric materials contain a multitude of useful properties in modern technology. For example, ferroelectrics have a high applicability in microelectronics: memories with random non-volatile access, capacitors, wave guides or IR detectors, sensorial devices, pyroelectric devices, piezoelectric devices.

### **1.4 Types of ferroelectric materials**

With a few exceptions, materials that dominate the market of piezoelectric devices are oxide solutions, based on lead: lead zirconate titanate  $Pb(Zr_{1-x}Ti_x)O_3$  - PZT and relaxator ferroelectrics such as  $(1-x)Pb(Mg_{1/3}Nb_{2/3})O_3 - xPbTiO_3$  - PMN-PT[2]. This type of material – PZT – with a few chemical modifications, is by far the most utilized piezoelectric material [3].

Even so, due to the toxicity of lead [4,5], investigations have commenced regarding substituting the materials that are based on it. These have been taking place ever since 1950, but it has not been until recent years, starting with the growth of consciousness regarding negative environmental effects, as well as legislative concerns [6], that the interest of worldwide researchers has increased towards developing and discovering piezoelectric and ferroelectric materials without lead [7,8,9].

## **Chapter 2: Deposition and characterization techniques of ferroelectric thin films**

### **2.1 Deposition techniques of ferroelectric films**

In the field of the science of materials, the almost infinite possibility to conceive new

combinations of materials with chemical, physical and mechanical properties different than the initial ones, has changed modern society. The miniaturization of electronic devices has become a great challenge for scientists, taking into account their great numbers. Modern technology requires the use of thin films for different applications such as ferroelectric non-volatile memories, devices of acoustic surface waves, pyroelectric devices etc. [10]

A thin film is defined as a material dimensionally reduced, created through the condensation of different atomic/molecular/ionic species of the matter, but having the same functionality as the initial volumetric material [11]. “Thin” is a relative term, and can vary according to the destination of the specific layer, but most technical deposition cases allow controlling the thickness of a thin layer around values of a few tens or hundreds of nanometers.

The properties of thin films depend on the deposition method. The principal methods through which thin films can be achieved are, according to the nature of the process, chemical, physical or mixt.

### **2.3 Utilized deposition techniques – PLD**

Thin PLZT and NBT films such as NBT-BT have been deposited, along the years, through a multitude of deposition techniques. The most important aspect in obtaining a thin film of good PZT is the conservation of a correct stoichiometry, more specifically the conservation of the lead content, which is easy to achieve when the method used is that of pulsed laser deposition – PLD.

In specialist literature, pulsed laser deposition always represents a succession of two processed: **the vaporization of a target-material which is followed by the deposition of the vapors on a collector – substrate located at a certain distance and placed, generally, in parallel with the target.**

The representation of the ablation installation for PLD is sketched in figure 2. A laser fascicle uniformly irradiates the target, and through an optimum selection of the work parameters, such as the wave length, fluency, the gas in the work environment and its pressure, the substrate temperature and the distance between the target and the substrate, it is possible to control the quality of the deposited films, even in the case of a certain complex stoichiometry.



The material ablated with the laser, being under expansion in the form of plasma, can be collected on a substrate in order to obtain thin films.

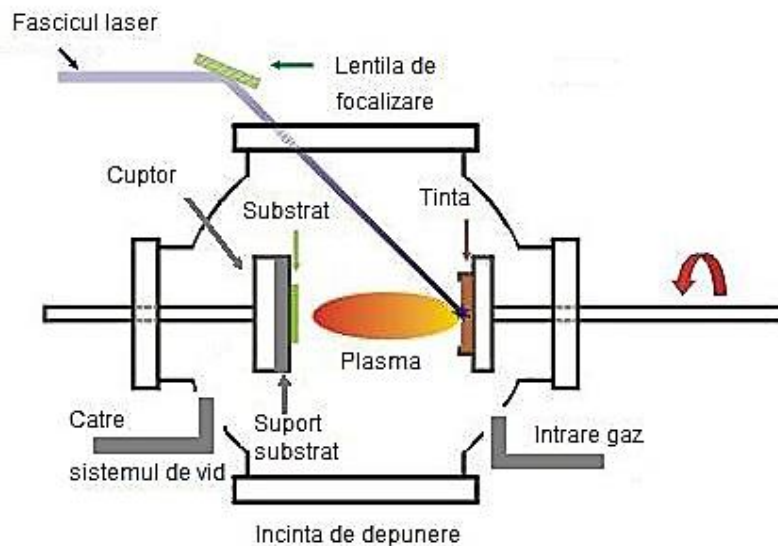


Figure 2: Schematic representation of the pulse laser deposition system [12]

The deposition precincts contain a support for the target and a support for the sub-layer, and are equipped with a vacuum system. For the deposition of thin multi-layer films, the support for the target has the aspect of a carrousel which contains multiple targets. Normally, the target support is continuously rotated and translated during the deposition.

The sub-layer, placed in parallel with the target, can be heated, the ovens in our laboratories reaching values of up to 750°C. The pressure in the deposition room can reach up to  $10^{-6}$  mbar. A laser of great strength is utilized as a source of external energy for the vaporization of the material and the deposition of thin films.

The choice of laser and establishing its function parameters (wave length, fluency, the frequency of pulse repetitions, the duration of the laser pulse) depend on the physical properties of the target which must, as a primary condition, absorb the laser radiation.

In conclusion, the pulsed laser deposition technique is simple from a technological point of view, being one of the most accessible methods of obtaining thin films from the point of view of the experimental device. Mechanisms that lead to the ablation and the deposition of material on the substrate depend both on the laser characteristics, as well as the optical, morphological and thermodynamic properties of the target material.

### **2.3 Characterization methods of ferroelectric thin films**

As shown in this paper, I have utilized as a deposition method the pulsed laser ablation. The following section will also contain a brief presentation of some of the experimental methods utilized for the analysis of the properties of thin layers obtained through the deposition method discussed.

For the analysis of the morphology of thin ferroelectric film surfaces obtained, there have been used the following characterization techniques: atomic force microscope, scanning electron microscope and spectral ellipsometry. For the analysis of the structure of the thin ferroelectric films obtained, X-XRD ray diffraction has been used, as well as the transmission electron microscope (TEM). In order to study the dielectric, piezoelectric and ferroelectric properties of the thin films obtained, dielectric spectroscopy and atomic piezoelectric force microscope (PFM) were utilized.

### **Chapter 3: Deposition and characterization of thin ferroelectric film with lead PLZT**

Lead zirconate titanate doped with lanthanum (PLZT), member of the ferroelectric family, represents a very interesting class of materials with optic and optoelectronic applications, due to its increased transparency, its wide range of compositions and its remarkable electro-optic properties. PLZT is utilized on a large scale in electro-optic applications and is characterized by a large dielectric anomaly, around 24°C (room temperature) for concentrations higher than the critical limit. Through the doping with lanthanum of lead zirconate titanate, properties superior than that of PZT are obtained: a higher dielectric constant, a smaller coercive field and high electro-mechanic gearing coefficients.

Thus, this chapter has focused on studying the influence of different deposition parameters: the temperature of the sub-layer, the RF influence, the wave length, the laser fluency, etc. on the film's properties, selecting for our investigations the composition  $(\text{Pb}_{1-3x/2}\text{Lax})(\text{Zr}_{0.2}\text{Ti}_{0.8})\text{O}_3$  with  $x = 0,22$  (PLZT 22/20/80), as can be seen in the phase diagram from figure 3.

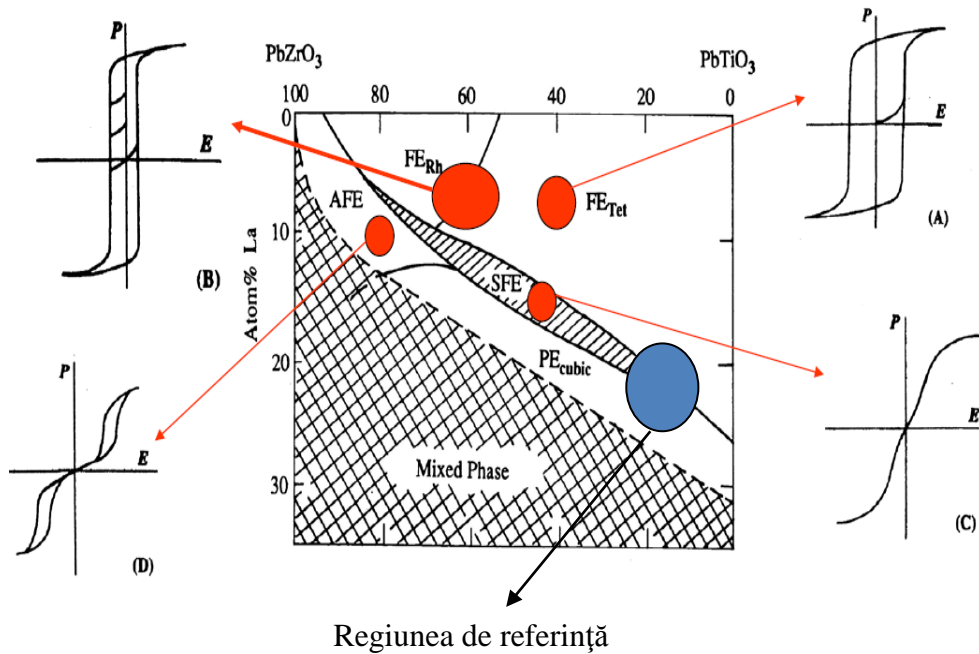


Figure 3. Typical hysteresis curves obtained for PLZT, having diverse compositions for diverse applications: a) FE linear memories; b) NVFRAM memories; c) SFE slim-loop memories; d) anti-ferroelectric behavior [13]

The emphasis was placed on the electro-optic behavior of these films, integrated in a heterostructure TCO/ ferroelectric/ conductive substrate.

### 3.1 Experimental conditions

Thin PLZT 22/20/80 films were deposited on different sub-layers – SRO/STO and STON, through the PLD method [14,15]. The growth of PLZT films was achieved utilizing an ArF laser at the wave length of 193 nm and a frequency of 10 Hz, with a value for the laser fluency of 1,8 J/cm<sup>2</sup>. The target-sub-layer distance was maintained at 50mm in order to obtain thin, high quality PLZT films, with a duration for the deposition of 60 min.

### 3.2 Results and discussion

From the AFM images (Fig. 4a) b)) it is noticeable that the type of thin sub-layer influences the morphology of films: those obtained on SRO/STO are more compact than the ones

obtained on Nb: STO. The film deposited on the STON sub-layer is uniform, with round crystallites of 300 nm; the ruggedness value is low, around 12 nm. Also, it has been noticed that the surface of the thin PLZ/SRO/STO film has a relatively small ruggedness (around 7nm), without drops or other defects.

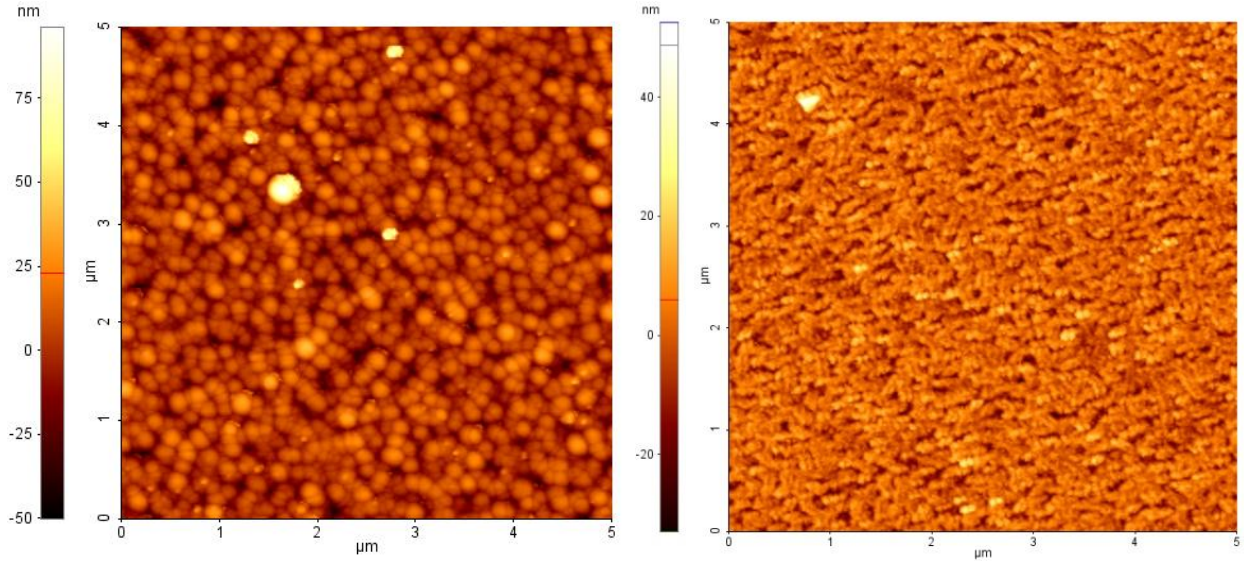


Figure 4. The AFM images of thin PLZT 22/20/80 films deposited on: a) Nb: STO, RMS=11.5nm; b) SRO/STO, RMS=7nm

Figure 5 presents the XRD spectrums of thin PLZT 22/20/80 films, deposited on STON. It can be noticed that the STON sub-layer induced a growth direction oriented on the c axis. The cubic network parameters – 3.991 Å for the Nb film: STO – have almost of the same value as the volume form of 3.987 Å PLZT, which indicates the fact that PLZT films are relaxators and the stoichiometry is similar to the chemical composition of the target, also confirmed by mass spectroscopy experiments on secondary ions (SIMS) [14].

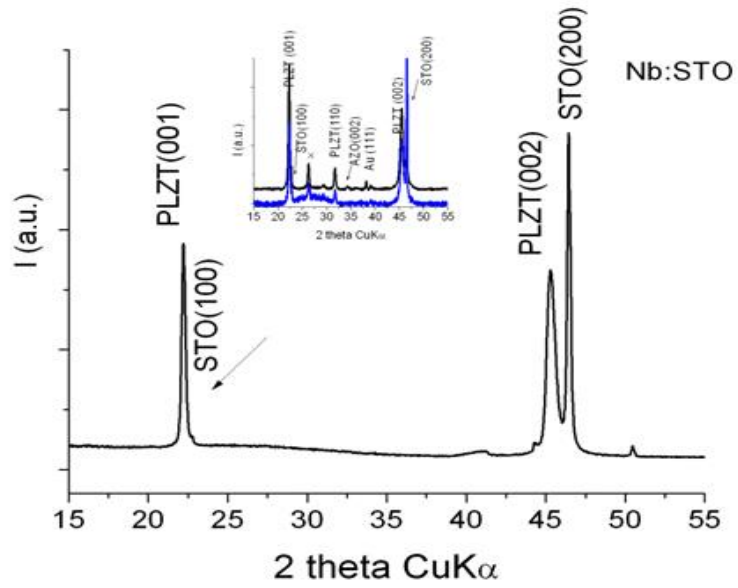


Figure 5. XRD spectrums of the thin PLZT 22/20/80 films deposited on Nb:STO

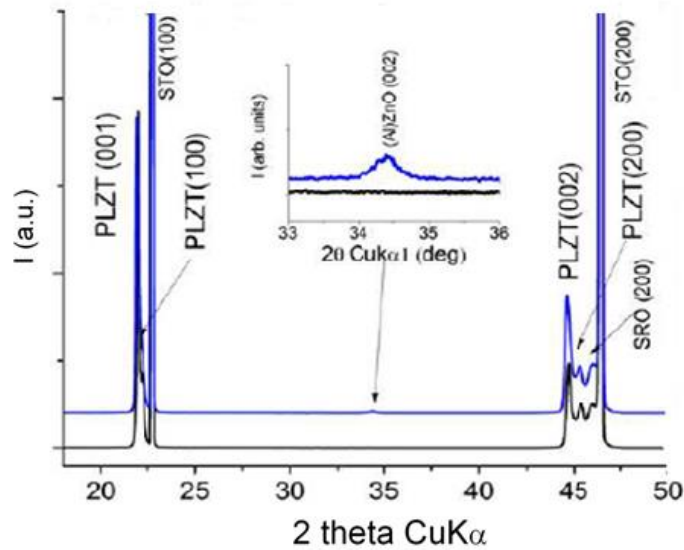


Figure 6. XRD spectrums of the thin PLZT 22/20/80 films deposited on SRO/STO substrate, before and after the deposition of AZO

Figure 6 presents the out-of-plane  $2\theta / \omega$  diffraction spectrums of thin PLZT films, before and after the Al: ZnO (AZO) deposition. The films only present reflections (h00) / (001), without other parasite drops, for example, (101). The XRD spectrum of the thin film, after the

AZO deposition, reveals the same structural characteristics of the PLZT, as well as the presence of supplementary  $\text{Zn(A1)O(002)}$ .

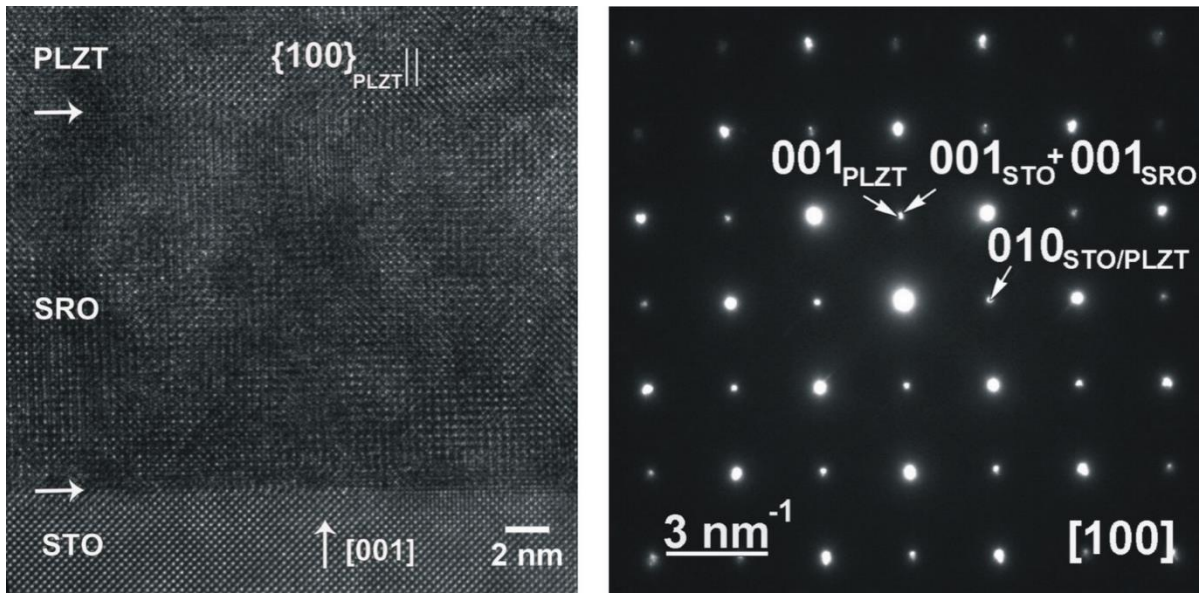


Figure 7 (a). The HRTEM image of the PLZT/SRO/STO multi-layer structure; (b) SAED model recorded on the PLZT/SRO/STO multi-layer structure (corresponding to image (a))

Figure 7, the HRTEM image of the PLZT/SRO/STO multi-layer structure demonstrates an epitaxial growth, and the excellent quality of the STO/SRO and SRO/PLZT interfaces. The SAED image confirms, in addition, the epitaxial growth of the PLZT and SRO layers on the STO (001) sub-layer (Fig. 7b). With regards to the X-ray diffractogramme, the pseudo-cubical cell was utilized for SrRuO<sub>3</sub> (instead of orthorombic), for calibrating the diffraction.

For testing the ferroelectric properties in thin PLZT films, the atomic force microscope was utilized, on piezo mode. Thin PLZT films (22/20/80) present good piezoelectric properties, as can be noticed in Fig. 8. The measured values of the effective piezoelectric coefficient, with the greatest value being that of  $d_{33\text{eff}} \approx 35 \text{ pm / V}$ , are slightly smaller than the  $d_{33\text{eff}} \approx 50 \text{ pm / V}$  value measured on the thin PZT 20/80 layers, deposited on SrTiO<sub>3</sub> sub-layers [16].



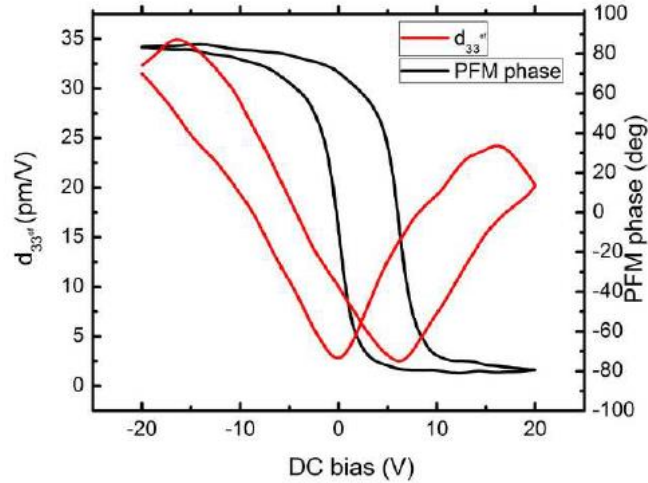


Fig. 8. The piezo measurements of thin PLZT/SRO/STO films

The permittivity and the dielectric losses of thin films deposited on a PLZT/SRO/STO sub-layer, measured in the range of frequencies 100 Hz – 1 MHz, are presented in Fig. 9a [15]. Comparatively, the values of the constant, and the dielectric losses of a thin PLZT film deposited on another type of electrode (Pt/Si) are presented. As can be observed, besides the high values of the dielectric losses and the low ones of the dielectric constant, a strong dielectric relaxation maximum for PLZT/SRO/STO appears at approximately 100 kHz, despite the excellent structural and compositional properties.

Fig. 9b presents the primitive variation of the dielectric losses with a temperature at different frequencies. The strong growth of dielectric losses, over  $T = 450$  K, especially at a lower frequency, is due to the contribution of conductivity. Indeed, there is a strong dc conductivity component measured at  $T = 454$  K, representing the interior of the figure. The wide peak of the  $\epsilon$ - $T$  curves indicates the phase transition from the paraelectric to the ferroelectric of the PLZT film, which is located approximately 140 K from the top of the susceptibility temperature  $T_{mb}$  in the evidence of volumetric form.

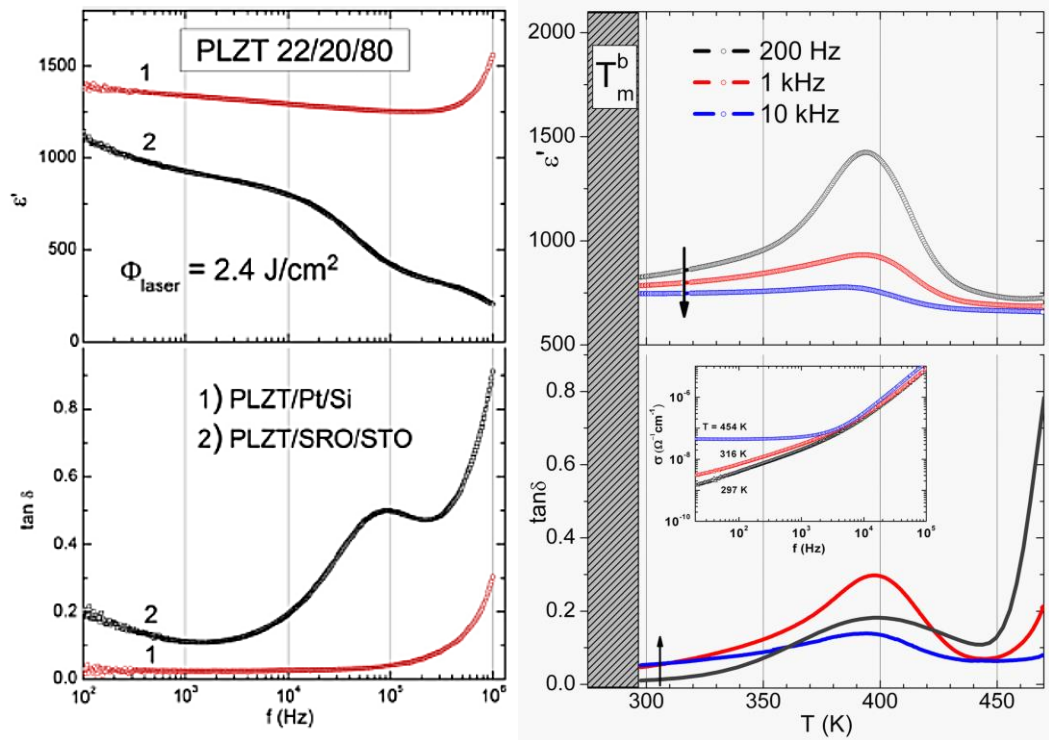


Figure 9 (a) The dielectric permittivity spectrums of PLZT films deposited on SRO/STO. Comparatively, the dielectric properties of a thin PLZT/Pt/Si film; (b) The permittivity and dielectric losses variation with the temperature for different frequencies measures on the PLZT film.  $T_m^b$  represents the maximum dielectric permittivity temperature measured in a volumetric form, whilst the arrows indicate the growth of the signal's frequency. Inside the figure, the variation of alternative current with a different temperature frequency is presented.

Electro-optic investigations were further achieved through measurements of the spectral ellipsometry. The measurements were done between 300 nm and 1200 nm in the spectrum without an applied electric field, at a fixed angle of incidence, in order to obtain the classical ellipsometry angles  $\Psi$  (amplitude) and  $\Delta$  (phase) as an energy function.

The electro-optic behavior of thin PLZT/Nb: STO films, for  $\lambda = 540$  nm, a polar incidence angle of  $65^\circ$ , with a calculated value for the refraction index of approximately  $n=2,26$ , is presented in Fig. 10.



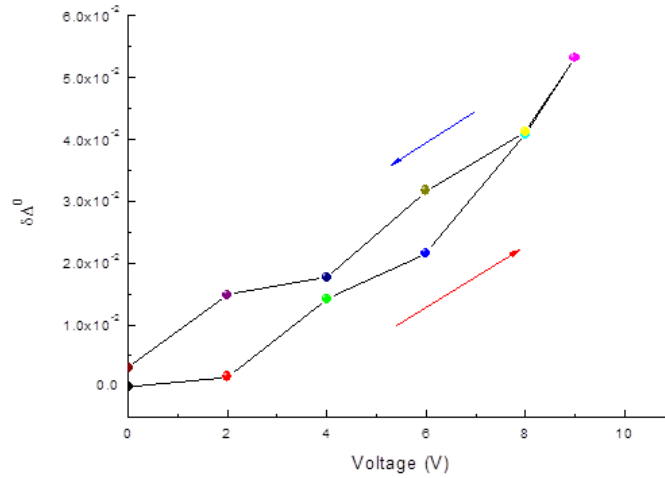


Figure 10. Birefringence shift as a function of applied dc fields at  $\lambda = 540$  nm and a polar angle of  $65^\circ$  incidence for the PLZT 22/20/80 thin films deposited on Nb: STO

The square coefficient of the electro-optic effect can be calculated with the formula:

$$R = \frac{\delta\Delta\lambda}{\pi n^3 E_z^2 d}$$

where  $\delta\Delta$  is the relative phase shift in rad,  $\lambda$  is the wave length,  $n$  is the refraction index of the film,  $E_z$  is the electric applied field and  $d$  is the thickness of the film in nm. The calculated value is  $R = 0,331 * 10^{-17} \text{ m}^2/\text{V}^2$ , a value relatively small compared to the value in a volume format, but still much greater for materials utilized as industrial standards, for example -  $\text{KTaO}_3$  este de  $0,21 * 10^{-17} \text{ m}^2/\text{V}^2$ . [14,17]

## Conclusions

The square electro-optic behavior and the dielectric properties of thin  $\text{Pb}_{1-3x/2}\text{La}_x\text{Zr}_{0.2}\text{Ti}_{0.8}\text{O}_3$ ,  $x = 0,22$  (PLZT 22/20/80) films deposited on Nb: STO and SRO/STO sub-layers were studied. Thin ferroelectric PLZT films were obtained through pulsed laser deposition. The structural and compositional tests show the epitaxial nature of the films, alongside a stoichiometry that is conserved along the thickness of the films.

For both types of utilized sub-layers a very good structural quality was noted, the XRD

and TEM measurements confirming the epitaxial way of PLZT layer growth. The ferroelectric measurements have demonstrated typical properties of a relaxator material, for the PLZT 22/20/80 composition. Utilizing spectral ellipsometry as a measurement technique, the electro-optic behaviors for thin PLZT layers deposited on the two types of sub-layers were determined. If in the case of layers deposited on STON, the electro-optic behavior is of quadratic-Kerr type, with the value of the square electro-optic coefficient being  $0.331 * 10^{-17} \text{ m}^2/\text{V}^2$ , in the case of the samples deposited on SRO/STO the electro-optic behavior is linear due to the additional deformation introduced in the thin PLZT layer by the SRO support used.

## Chapter 4: Deposition and characterization of ferroelectric thin films without lead – NBT

Perovskite ferroelectric materials based on  $\text{Na}_{0.5}\text{Bi}_{0.5}\text{TiO}_3$  (NBT) are considered among the most promising materials able to substitute  $\text{Pb}(\text{Zr}_{1-x}\text{Ti}_x)\text{O}_3$  (PZT) - in the devices designed to meet the standards and environmental legislation[18]. Sodium and bismuth titanate is classified as material with perovskite structure ( $\text{ABO}_3$ ) in which the nodes in position A consist of a mixture of  $0.5 \text{ Bi}^{3+}$  and  $0.5 \text{ Na}^{1+}$  cations as observed in Figure 11. Since its discovery by the researcher Smolensky, in 1960 [19], its physical properties and crystal structure or phase transitions have been extensively studied.

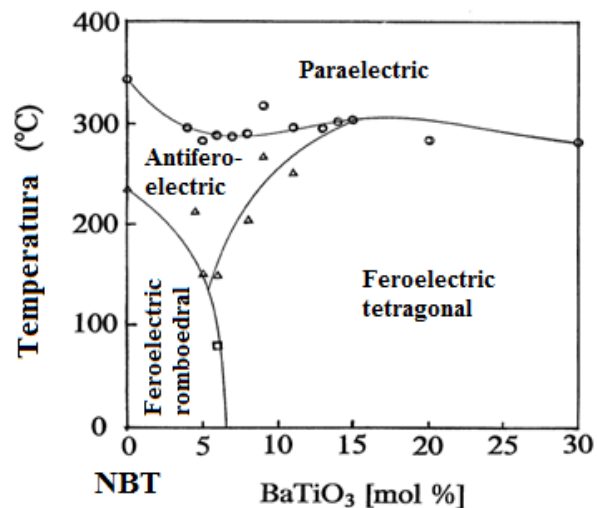
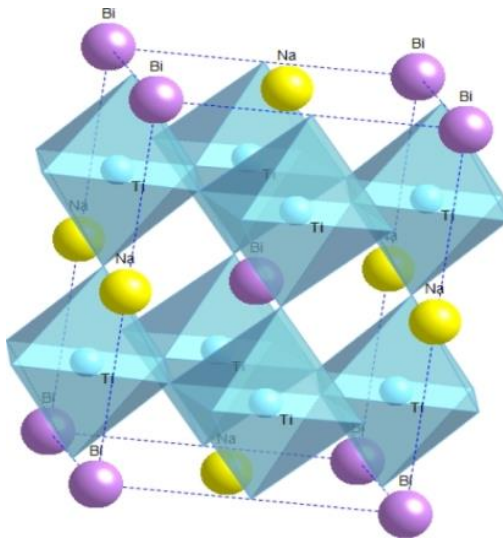


Figure 11: a. The pseudo-cubic structure of  $\text{Na}_{0.5}\text{Bi}_{0.5}\text{TiO}_3$  (NBT) [20]. b. The phase diagram of the  $(1-x)\text{NBT} - x\text{BT}$  in which there are highlighted the morphotropic phase boundaries, between the two ferroelectric phases: rhombohedral and tetragonal [21]

The perovskite compound  $(1-x)\text{Na}_{0.5}\text{Bi}_{0.5}\text{TiO}_3 - x\text{BaTiO}_3$ , shows a morphotropic phase boundary (Morphotropic Phase Boundary - MPB) between the rhombohedral and tetragonal phase for values of  $x = 0.06$  to  $0.07$  (Figure 11b), around which the properties of this material improve considerably ( $T_C = 320^\circ\text{C}$ ,  $d_{33} \sim 450$  pC/N). Relative deformation is up to 85%, which shows the dependence of the ferroelectric properties of the composition  $(1-x)\text{NBT} - x\text{BT}$  to the content of  $\text{BaTiO}_3$  [22,23,24,25].

#### **4.1 Experimental conditions**

To obtain the NBT and NBT-BT films, the pulsed laser deposition technique was used (PLD), starting from targets with a composition of  $(1-x)\text{NBT}-x\text{BT}$  ( $x=0$  and  $0.06$ ). For the deposition of films, a Surelite II Nd: YAG laser was used, with a wavelength of 265 nm, a pulse duration of 5 ns and a frequency of 10 Hz. Laser fluency was set at  $1.6 \text{ J/cm}^2$ . For growing the thin films of  $(1-x)\text{NBT}-x\text{BT}$  with a high degree of crystallinity, oriented (001), there have been used commercial platinum substrates deposited on silicon ( $\text{Pt/TiO}_2/\text{SiO}_2/\text{Si}$ ), placed at a distance of approximately 4.3 cm from the target.

#### **4.2 Results and discussions – Comparison between the NBT and NBT-BT6**

I investigated through atomic force microscopy the growth mode of thin films of NBT and NBT-BT6 on substrates of  $\text{Pt/TiO}_2/\text{SiO}_2/\text{Si}$  because they are relatively inexpensive and can be used on electrical measurements.

From the AFM images (Figure 12) obtained on NBT films, there was noticed that those deposited from the NBT target have a continuous and relatively uniform appearance, without drops or "droplet" formations, with roughness of approximately 30 nm, while those obtained from the NBT-BT6 target (Figure 13) show a quite different morphology with roughness of approximately 40 nm.

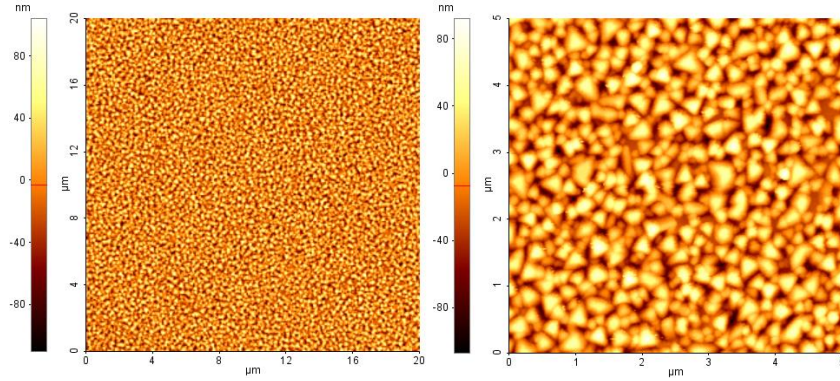


Fig. 12 The AFM images of the NBT films deposited on substrates of Pt/TiO<sub>2</sub>/SiO<sub>2</sub>/Si at 730°C. The surfaces in the images are areas of 20x20 μm<sup>2</sup>(a) and 5x5 μm<sup>2</sup>(b).

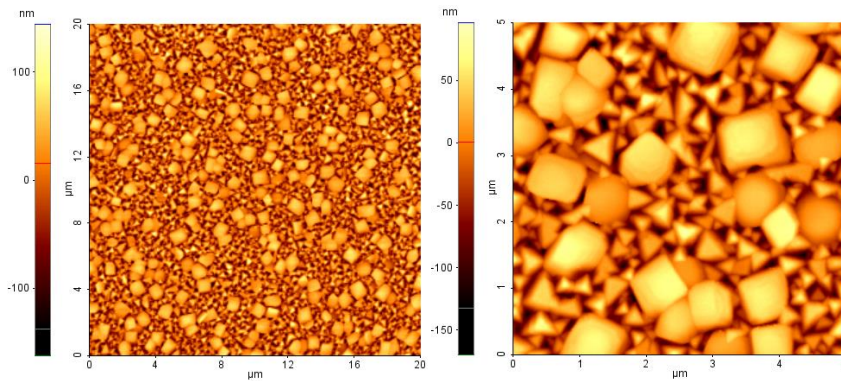


Fig. 13 The AFM images of the NBT-BT6 films deposited on substrates of Pt/TiO<sub>2</sub>/SiO<sub>2</sub>/Si at 730°C. The surfaces in the images are areas of 20x20 μm<sup>2</sup>(a) and 5x5 μm<sup>2</sup>(b).

X-ray spectra on NBT and NBT-BT6 targets and films deposited on Pt/TiO<sub>2</sub>/SiO<sub>2</sub>/Si are shown in Figure 14 a. The NBT target spectrum shows a typical rhombohedral structure that can be described as a pseudo-cubical cell ( $\alpha = 89.8^\circ$ ) with a value of the network parameter  $a=3.89\text{\AA}$ . This is identical to the standard value for this material. On the same graph, it is noticed that the model matches the NBT film grown on Pt/TiO<sub>2</sub>/SiO<sub>2</sub>/Si.

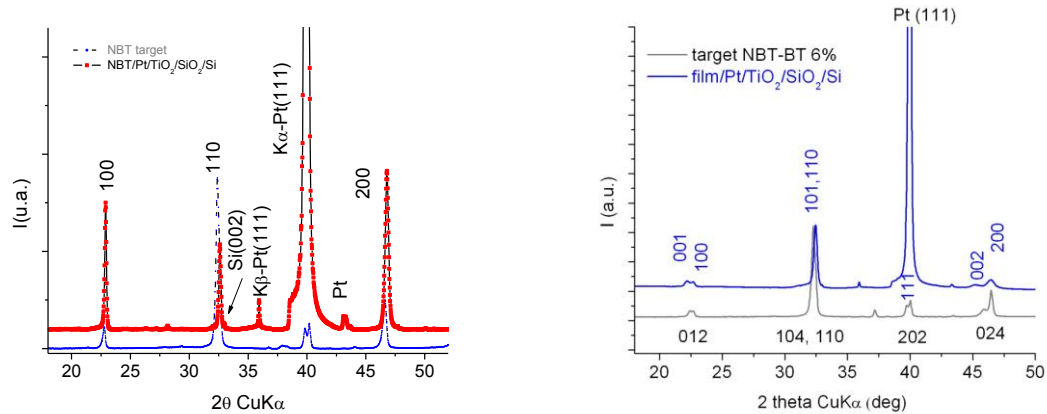


Fig. 14.a. The XRD spectrum of the NBT sample deposited on a substrate of Pt/TiO<sub>2</sub>/SiO<sub>2</sub>/Si. The bottom spectrum corresponds to the target. b. The XRD spectrum of the NBT-BT6 sample deposited on a substrate of Pt/TiO<sub>2</sub>/SiO<sub>2</sub>/Si. The bottom spectrum corresponds to the target.

Studies on NBT-BT6 thin films (Fig. 14.b.) showed that they depend critically on the composition and oxygen pressure during deposition: small variations in this parameter induce structural changes to the emergence of various parasitic stages.

I showed that the films obtained from NBT target exhibit excellent values of the dielectric permittivity, greatly improved compared to the values reported in volume form until now. Frequency dispersion is somewhat higher, but the dielectric constant values are much higher than in volume form, nearly 1560 to 1 kHz (compared to 700 in volume). In case of NBT-BT films, the dielectric constant value at 1 kHz is higher for thin films ( $\epsilon_r \sim 2500$ ), in comparison with the volume form ( $\epsilon_r \sim 1850$ ), while, at the frequency of 10 kHz, the values obtained are similar ( $\epsilon_r \sim 1800$ ) for both types studied (thin film and volume form). Dielectric loss ( $\text{tg } \delta$ ) are higher for both compositions, both for NBT and NBT-BT6, for thin films in contrast to volume form.

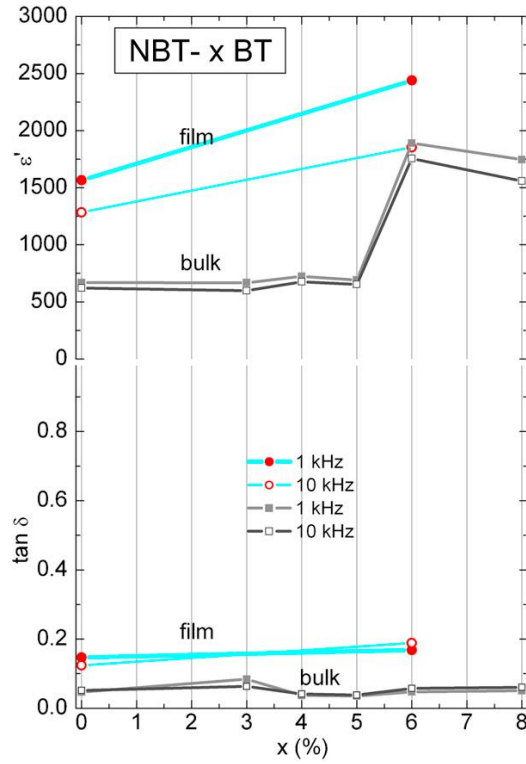


Fig. 15: The values of dielectric constants and dielectric losses for NBT and NBT-BT6 in thin films and bulk.

#### 4.3 Results and discussions – characterization of NBT-BT6 films

Following the investigations on the two compositions, NBT and NBT-BT6, we conclude that the dielectric properties are superior in case of films obtained from the NBT-BT6 doped target, compared to the films obtained from NBT undoped targets and also clearly superior to certain compositions based on PZT lead.

From the AFM images (Figure 16) we were able to distinguish predominantly triangular looking crystallites at 730°C, with predominantly rhombohedral faceted aspect at 650°C and a mixture of the two for the samples obtained at 700°C.

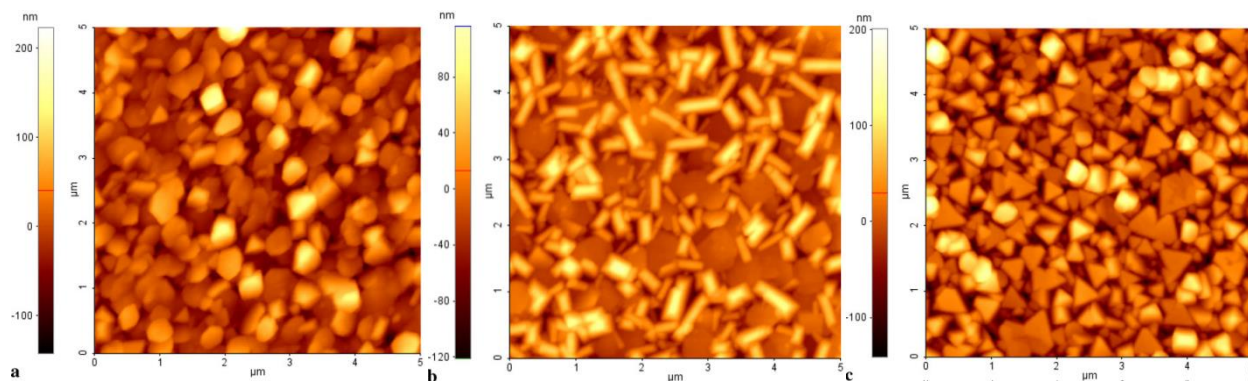


Fig. 16 The AFM images of the NBT-BT6 films deposited on substrates of Pt/TiO<sub>2</sub>/SiO<sub>2</sub>/Si at different temperatures: a. 650 °C, b. 700 °C, c. 730 °C. The surfaces in the images are areas of 5x5 μm<sup>2</sup>.

Figure 17 shows the XRD spectra of the NBT-BT6 films deposited at three different temperatures, 650°C, 700°C and 730°C, in comparison with that of the target used. The spectra indicate the formation of polycrystalline films with random orientation whose phase structure is strongly dependent on the substrate temperature. We note that the XRD spectrum of the NBT-BT6 target corresponds to a mixture of phases between the R3c rhombohedral one and the P4mm tetragonal one, as shown by splitting the peaks (111) and (200), (012) and (024) in the model below in Fig. 17 [26].

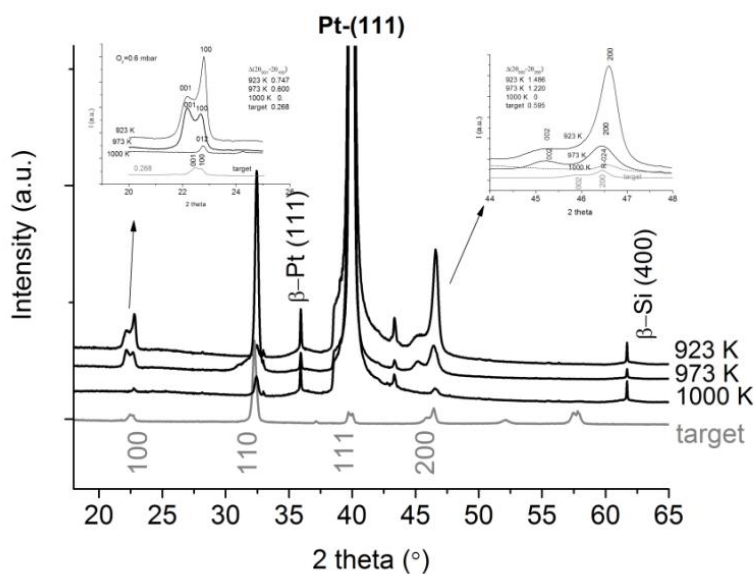




Fig. 17 The XRD spectrum of the NBT-BT 6% samples deposited on a layer of Pt/TiO<sub>2</sub>/SiO<sub>2</sub>/Si at different temperature (650°C, 700°C and 730°C). The bottom spectrum corresponds to the target.

Correlating the AFM images with the spectra obtained, we can say that the triangular forms present at 730°C induce the presence of a maximum/peak (111), while the square or rectangular crystallites present at 650°C and 700°C correspond to the maximums (100) and (110).

In order to determine the dielectric, piezoelectric and ferroelectric properties, on the surface of the investigated films, circular electrodes of Au (with an area of 0.22 mm<sup>2</sup>) were deposited using a mask, the lower electrode being Pt. The local values measured of the  $d_{33}^{eff}$  ( $\approx$  83 pm/V) are even higher than those previously reported for NBT or for lead-based thin films, such as Pb (ZrTi)O<sub>3</sub> or PbTiO<sub>3</sub> [i]. However, these values of the  $d_{33}^{eff}$  are lower than those of ceramics in volume form NBT-BT6, which are reported to be 100 pm/V.

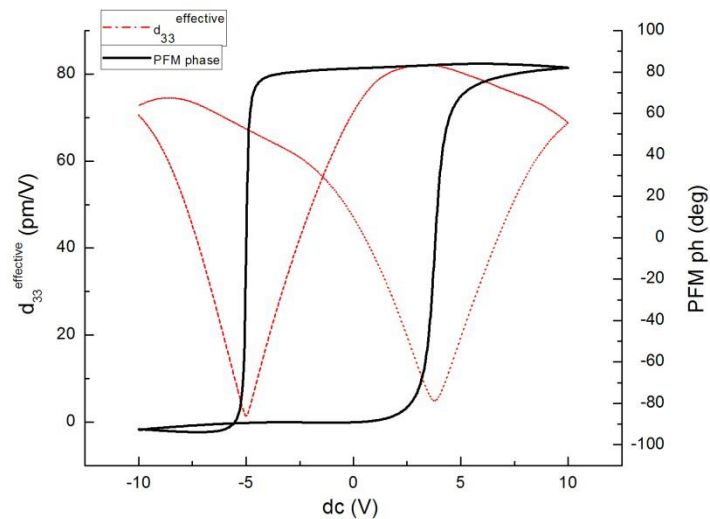


Fig. 18 Piezoelectric response measurements performed on NBT-BT6 films.

In Fig. 19, there were compared the dielectric properties of the NBT-BT6 films deposited on Pt/TiO<sub>2</sub>/SiO<sub>2</sub>/Si at different temperatures of the substrate (650°C and 730°C) in the frequency range of 100 Hz-1 MHz. Films grown at 650°C have a higher dielectric constant ( $\epsilon' \sim 1000$ ), while



films grown at 730°C have smaller values ( $\epsilon'' \sim 700$ ). The values of dielectric loss are, however, comparable in the two samples and similar to bulk values.

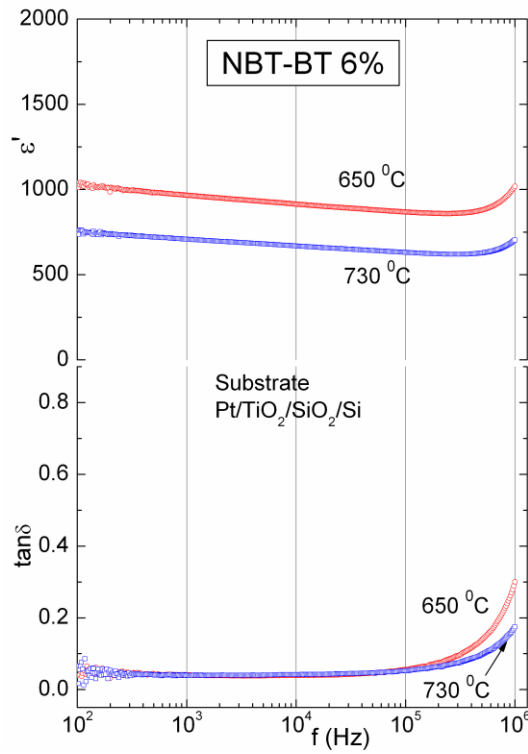


Fig. 19. The dielectric constant  $\epsilon'$  at room temperature and  $\tan \delta$  loss variation with frequency in case of NBT-BT6 films deposited at different temperatures on Pt/TiO<sub>2</sub>/SiO<sub>2</sub>/Si.

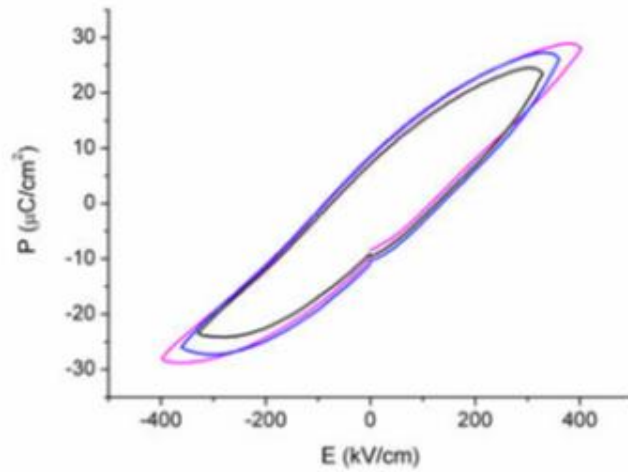


Fig. 20. Electrical hysteresis curve for a NBT-BT6 film deposited on Pt/TiO<sub>2</sub>/SiO<sub>2</sub>/Si

Hysteresis measurements of NBT-BT6 films deposited on Pt/TiO<sub>2</sub>/SiO<sub>2</sub>/Si are shown in Fig. 20. The spontaneous polarization was about 30  $\mu\text{C}/\text{cm}^2$  and the residual polarization, about 10  $\mu\text{C}/\text{cm}^2$ . The relatively high value of the coercive field (100 kV/cm) could be explained by the presence of internal stress and structural defects.

#### 4.4 Conclusions

In this chapter, I investigated the role of the deposition temperature, as well as the amount of BT dopant present in the target on the structure and morphology, but also the dielectric and piezoelectric properties of thin films of NBT and NBT-BT6 obtained by pulsed laser deposition.

We have shown that the structural and dielectric properties of NBT-BT thin films with composition at the morphotropic phase boundary (6% BT) depend critically on the composition and oxygen pressure during deposition: small variations in this parameter induce structural changes to the emergence of various parasitic stages.

The films obtained from NBT targets show excellent values of dielectric permittivity, greatly improved compared to the values reported in volume form until now. The frequency dispersion is somewhat higher, but the dielectric constant values are much higher than in volume form, nearly 1560 to 1 kHz. Regarding the composition of NBT-BT 6, thin films obtained show a very high dielectric constant, as expected, but with more frequent dispersion behavior. Dielectric loss values are larger than in volume form, but the dielectric constant values were 2500 to 1 kHz, while at 10 kHz it is similar to the one reported for bulk - 1800.

After fathoming investigations on NBT-BT6 thin films, we showed that their structural and dielectric properties depend critically on the substrate temperature during deposition. From AFM images, there can be distinguished predominantly triangular-looking crystallites at 730°C, with predominantly rhombohedral faceted aspect at 650°C and a mixture of the two for samples obtained at 700°C. The films deposited at lower temperatures show a splitting of the maximums/peaks (100) and (200) which announces the formation of a structure in the border region of morphotropic phase transition rhombohedral-tetragonal, in which the two coexist. In the film deposited at 650°C the tetragonal peaks are more intense, indicating a preferred

orientation in the direction (100) while in the film obtained at 730°C there is a single phase, the rhombohedral one, respectively.

Moreover, the NBT-BT6/Pt/Si thin films exhibit a classical switching behaviour, the piezoelectric hysteresis confirming the piezoelectric and ferroelectric characteristics. Local values measured of the  $d_{\text{eff}}^{33}$  ( $\approx 83$  pm/V) are even higher than those previously reported for NBT or lead-based thin films. Spontaneous polarization was about  $30 \mu\text{C}/\text{cm}^2$  and the residual polarization of about  $10 \mu\text{C}/\text{cm}^2$ .

## General conclusions

In this thesis, I aimed to obtain PLZT thin films with optical, electro-optical and dielectric properties similar or even higher than those present in the volume form, in order to integrate them into compact electro-optical devices. The use of electro-optical devices based on PLZT can reduce the toxic effects on the environment produced by the use of lead zirconium titanate (PZT-high content of lead) by doping them with lanthanum. By depositing thin films of NBT and NBT-BT, considered potential alternative materials to be used in microelectronics instead of PZT, I tried to investigate the role of certain experimental conditions of deposition on the crystalline structure, the dielectric properties, phase transition temperature and dielectric stability limits. Therefore, the influence of different deposition parameters on the properties of perovskite ferroelectric thin films was investigated:

- a.  $(\text{Pb}_{1-3x/2} \text{La}_x)(\text{Zr}_{0.2}\text{Ti}_{0.8})\text{O}_3$  with  $x = 0,22$  (PLZT 22/20/80) - lead zirconate titanate doped with lanthanum
- b.  $\text{Na}_{0.5}\text{Bi}_{0.5}\text{TiO}_3 - x\text{BaTiO}_3$  with  $x = 0$  and  $6$  (NBT and NBT-BT 6) – sodium and bismuth titanate, doped with barium titanate

The main results presented herein, as well as the original contributions, can be summarized as follows:

I. **I deposited piezoelectric thin films of PLZT 22/20/80**, by pulsed laser deposition method, from a ceramic target with the composition of  $(\text{Pb}_{0.67}\text{La}_{0.22})(\text{Zr}_{0.2}\text{Ti}_{0.8})\text{O}_3$ , in the oxygen atmosphere, on STON and SRO/STO substrates. I used an ArF laser at a wavelength of 193 nm and a frequency of 10 Hz, with a value of the laser fluence of  $1.8 \text{ J}/\text{cm}^2$ , while the target-substrate distance was maintained at 50 mm.

1. I analyzed the films deposited by optical microscopy, noticing that the type of substrate influences the morphology the films: those obtained on SRO/STO are more compact than those obtained on Nb: STO. The film deposited on the STON substrate is uniform, with round crystallites with dimensions of 300 nm; the roughness value is low, about 12 nm. I have also noticed that the surface of the PLZT / SRO / STO thin film has a relatively small roughness (about 7 nm), without drops or other defects.

2. I performed X-ray diffraction analysis on PLZT films which showed that the STON substrate induces c-axis oriented growth (direction) and that they are relaxors and the stoichiometry is similar to the chemical composition of the target, as confirmed by experiments of mass spectroscopy of secondary ions (SIMS). Furthermore,  $\Phi$  scans of the PLZT film on SRO(100) / STO(100) show the plane orientation relationship between the film and the double substrate, resulting in the epitaxial growth of the films.

3. I demonstrated the epitaxial growth and the excellent quality of the interfaces by means of cross-sectional scanning electron microscopy (SEM), transmission electron microscopy (TEM) and electron diffraction (SAED), as well as atomic force microscopy studies (AFM). PLZT thin films on both substrates increased at the same time with the c-axis of the elementary cell perpendicular to the substrate, prerequisite for the films to exhibit high piezoelectric properties.

4. I investigated, using mass spectrometry of neutral atoms (SNMS), the chemical composition of PLZT thin films deposited on the SRO / STO substrate, in order to verify the stoichiometry of the samples. The Pb content was constant, with good correlation between the lead content of the stoichiometric target and the films obtained.

5. I tested the ferroelectric properties of the films using the atomic force microscope in piezo mode; they exhibit good piezoelectric properties, with measured values of the effective piezoelectric coefficient of  $d_{33}^{\text{eff}} \approx 35 \text{ pm} / \text{V}$ .

6. I measured the dielectric permittivity and loss of thin films deposited on SRO / STO measured in the frequency range 100 Hz - 1 MHz. Despite the excellent structural and compositional properties, in addition to the high values of dielectric loss and low value of the

dielectric constant, I noticed that at about 100 kHz a strong dielectric relaxation peak occurs for PLZT / SRO / STO.

7. I used the spectro-ellipsometry measurement technique to determine the behavior of electro-optical films deposited on both types of substrate. If in the case of layers deposited on STON, the electro-optical behavior is of the quadratic-Kerr type, with a value of the quadratic electro-optic coefficient of  $0.331 * 10^{-17} \text{ m}^2/\text{V}^2$ , in the case of samples deposited on SRO/STO the electro-optical behavior is linear, due to additional strain introduced in the PLZT thin layer by the SRO interlayer used.

All of the above confirm the outstanding electro-optical and piezoelectric properties of PLZT thin films obtained by pulsed laser deposition method.

II I have obtained NBT and NBT-BT6 films, with ferroelectric and piezoelectric properties, by pulsed laser deposition method, in oxygen atmosphere, at different pressures and different temperatures, using an Nd: YAG laser. To study the influence of the crystalline structure on the dielectric and ferroelectric properties of the thin films, I have used commercial platinum substrates deposited on silicon (Pt/TiO<sub>2</sub>/SiO<sub>2</sub>/Si), placed at a distance of about 4.3 cm from the target.

1. I investigated how to grow NBT and NBT-BT6 thin films on substrates of Pt/TiO<sub>2</sub>/SiO<sub>2</sub>/Si through atomic force microscopy. I noticed that those deposited from the NBT target show a continuous and relatively uniform aspect, without drops or "droplet" formations, with a roughness of approximately 30 nm, and those obtained from the NBT-BT6 target show a quite different morphology with a roughness of approximately 40 nm.

2. The study on the structural and dielectric properties of NBT-BT thin films with a composition at the morphotropic phase boundary (6% BT), showed that they depend critically on the composition and oxygen pressure during deposition: small variations of this parameter induce structural changes to the emergence of various parasitic stages.

3. I demonstrated that the films obtained from NBT target show excellent values of dielectric permittivity, greatly improved compared to the values reported in volume form until now. Frequency dispersion is somewhat higher, but the dielectric constant values are much

higher than in volume form, nearly 1560 to 1 kHz (compared to 700 in volume). In the case of NBT-BT films, the dielectric constant value for 1 kHz is greater for thin films ( $\epsilon_r \sim 2500$ ) compared to the volume form ( $\epsilon_r \sim 1850$ ), while, at the frequency of 10 kHz, the values obtained are similar ( $\epsilon_r \sim 1800$ ) for both types studied (thin film and volume form). Dielectric loss ( $\tan \delta$ ) is higher for both compositions, both for NBT and NBT-BT6, for thin films as opposed to volume form.

4. After fathoming investigations on NBT-BT6 thin films, I showed that their structural and dielectric properties depend critically on the substrate temperature during deposition. From AFM images, there can be distinguished predominantly triangular-looking crystallites at 730°C, with predominantly rhombohedral faceted aspect at 650°C and a mixture of the two for samples obtained at 700°C.

5. The X-ray diffraction studies have concluded that the films deposited at lower temperatures show a splitting of the peaks (100) and (200), which announces the formation of a structure in the border region of morphotropic phase transition rhombohedral-tetragonal, in which the two coexist. In the film deposited at 650°C, the tetragonal peaks are more intense, indicating a preferred orientation in the direction (100), while in the film obtained at 730°C, there is a single phase, the rhombohedral one, respectively.

6. I have shown that NBT-BT6/Pt/Si thin films exhibit a classical switching behaviour, the piezoelectric hysteresis confirming the piezoelectric and ferroelectric characteristics.

7. I have determined the piezoelectric constant  $d_{\text{eff}}^{33}$  ( $\approx 83$  pm/V), the values being even higher than those previously reported for NBT or lead-based thin films.

8. I have measured the spontaneous polarization which was about  $30 \mu\text{C}/\text{cm}^2$  and the residual polarization of about  $10 \mu\text{C}/\text{cm}^2$ .

All of the above confirm the piezoelectric and ferroelectric properties of NBT and NBT-BT6 thin films, obtained by pulsed laser deposition method.

The thesis presented is based on **a book chapter, a patent and 9 scientific articles published in ISI indexed journals:**

**Book chapter:** „Phase Transitions, Dielectric and Ferroelectric Properties of Lead-free NBT-BT Thin Films”, N. D. Scarisoreanu, R. Birjega, **A. Andrei**, M. Dinescu, F. Craciun, C. Galassi, Materials Science, "Advances in Ferroelectrics", Chapter 16, book edited by Aimé Peláiz Barranco, ISBN 978-953-51-0885-6, Published: November 19, 2012

**Patent:** „Metoda de producere a straturilor subțiri perovskitice fără plumb de titanat de sodium și bismut ( $Na_{0.5}Bi_{0.5}TiO_3$ ) cu proprietăți dielectrice înalte”, Scarisoreanu N., Dinescu M., **Andrei A.**, Birjega R., Monitorul Oficial al Romaniei, 2012

#### **Scientific works published:**

- **Lead-free ferroelectric thin films obtained by pulsed laser deposition**, N.D. Scarisoreanu, **Chis A.**, R. Birjega, C. Luculescu, F. Craciun, C. Galassi, M.Dinescu, APPLIED PHYSICS A-MATERIALS SCIENCE & PROCESSING, Volume: 101, Issue: 4, Pages: 747-751, 2010
- **Pulsed laser deposition of semiconducting double-doped barium titanate thin films on silicon substrates**, Apostol, I; Stefan, N; Birjega, R; Luculescu, CR; Andrei, A; Mihailescu, IN; METALURGIA INTERNATIONAL, Volume: 16, Issue: 4, Pages: 53-56, 2011
- **Silicon carbide thin films as nuclear ceramics grown by laser ablation**, M. Filipescu, G. Velisa, V. Ion, **A. Andrei**, N. Scintee, P. Ionescu, S.G. Stanciu, D. Pantelica, M. Dinescu, JOURNAL OF NUCLEAR MATERIALS, Volume: 416, Issue: 1-2, Pages: 18-21, 2011
- **Electrical and optical investigations on  $Pb_{1-3x/2}LaxZr_{0.2}Ti_{0.8}O_3$  thin films obtained by radiofrequency assisted pulsed laser deposition**, Scarisoreanu, ND; **Andrei A.**; Birjega, R; Pascu, R; Craciun, F; Galassi, C; Raducanu, D; Dinescu, M, THIN SOLID FILMS Volume: 520 Issue: 14 Special Issue: SI Pages: 4568-4571, 2012
- **Pulsed laser deposition of lead-free  $(Na_{0.5}Bi_{0.5})_{1-x}BaxTiO_3$  ferroelectric thin films with enhanced dielectric properties**, Andrei A.; Scarisoreanu, ND; Birjega, R; Craciun, F; Galassi, C; G. Stanciu; Dinescu, M, APPLIED SURFACE SCIENCE, Volume: 278, Pages: 162-165, 2013
- **Electro-optic and dielectric properties of epitaxial  $Pb_{1-3X/2}LaxZr_{0.2}Ti_{0.8}O_3$  thin films obtained by pulsed laser deposition**; Scarisoreanu, ND; Craciun, F; **Andrei, A**; Ion, V; Birjega, R; Moldovan, A; Dinescu, M; Galassi, C; THIN SOLID FILMS, Volume: 541, Pages: 127-130, 2013
- **Femtosecond laser ablation of  $TiO_2$  films for two-dimensional photonic crystals**, Anghel, I; Jipa, F; Andrei, A; Simion, S; Dabu, R; Rizea, A; Zamfirescu, M; OPTICS AND LASER TECHNOLOGY, Volume: 52, Pages: 65-69, 2013

- **Strain-induced long range ferroelectric order and linear electro-optic effect in epitaxial relaxor thin films**, Scarisoreanu, ND; Craciun, F; Birjega, R; Andrei, A; Ion, V; Negrea, RF; Ghica, C; Dinescu, M; JOURNAL OF APPLIED PHYSICS, Volume: 116, Issue: 7, Article Number: 074106, DOI: 10.1063/1.4893364, 2014
- **Characterization of zirconia thin films grown by radio-frequency plasma assisted laser ablation**, Cancea, V.N., Filipescu, M. , Velisa, G., Ion, V., Andrei, A., Pantelica, D., Birjega, R., Ionescu, P., Scintee, N., Dinescu, M., Romanian Reports in Physics, Volume 66, Issue 4, Pages 1137-1146, 2014

Furthermore, the results presented were disseminated in a large number of prestigious **international conferences** such as E-MRS (European Material Research Society Conference), COLA (International Conference on Laser Ablation), etc., also winning the '**Roger Kelly Award**' - **Young Researcher Competition** within the Summer School in Venice - III Venice International School on Lasers in Materials Science, SLIMS-2012.

### Selective Bibliography

- [1] A. Safari, R.K. Panda, V.F. Janas, *Ferroelectricity: Materials, Characteristics & Applications*, Key Engineering Materials, 122-124, 35, 1996
- [1] K.Uchino, *Ferroelectric Devices*, Volume 16 of Materials engineering, ISSN 1075-8577, CRC Press, 2000
- [1] B. Jaffe, W. R. Cook, H. L. Jaffe, *Piezoelectric ceramics*, Academic Press, 1971
- [1] Nevin R., *Environmental Research*, Volume 104, Issue 3, Pages 315–336, 2007
- [1] [http://en.wikipedia.org/wiki/Lead\\_poisoning](http://en.wikipedia.org/wiki/Lead_poisoning)
- [1] Official journal of the European Union, *Restriction of Hazardous Substances Directive 2002/95/EC, RoHS*, eur-lex.europa.eu, L37, pp. 19–23, 2003
- [1] Y. Saito, H. Takao, T. Tani, T. Nonoyama, K. Takatori, T. Homma, T. Nagaya, M. Nakamura, *Letters to Nature*, Nature432, 84-87, November 2004
- [1] P. K. Panda, Review: environmental friendly lead-free piezoelectric materials, *J Mater Sci*, 44:5049–5062, 2009
- [1] A. Westervelt, *Is that Lead in Your Lipstick?* FDA Tests Reveal Raised Lead Levels in U.S. Lipsticks, *Forbes*, <http://www.forbes.com/sites/amywestervelt/2012/02/07/is-that-lead-in-your-lipstick-fda-tests-reveal-raised-lead-levels-in-u-s-lipsticks>, 2012



- [1] A.R. West, *Solid State Chemistry and its Applications*, John Wiley & Sons, Singapore, 2003
- [1] K. Wasa, M. Kitabatake, H. Adachi, *Thin Film Materials Technology*, Sputtering of Compound Materials, Springer-Verlag, Germany, 2004.
- [1] [http://www.iqfr.csic.es/ql/Web\\_QL\\_english/Ablacion\\_laser](http://www.iqfr.csic.es/ql/Web_QL_english/Ablacion_laser)
- [1] G. H. Haertling, *PLZT electrooptic materials and applications*, Ferroelectrics, Volume 75, Issue 1, pages 25-55, 1987
- [1] N. D. Scarisoreanu, A. Andrei, R. Birjega, R. Pascu, F. Craciun, C. Galassi, D. Raducanu, M. Dinescu, *Electrical and optical investigations on  $Pb_{1-3x/2}La_xZr_{0.2}Ti_{0.8}O_3$  thin films obtained by radiofrequency assisted pulsed laser deposition*, Thin Solid Films 520, 4568, 2012
- [1] N. D. Scarisoreanu, F. Craciun, A. Andrei, V. Ion, R. Birjega, A. Moldovan, M. Dinescu, C. Galassi., *Electro-optic and dielectric properties of epitaxial  $Pb_{1-3x/2}La_xZr_{0.2}Ti_{0.8}O_3$  thin films obtained by pulsed laser deposition*, Thin Solid Films, 520, 4568–4571, 2012
- [1] Zhengkun Ma, F. Zavaliche, L. Chen, J. Ouyang, J. Melngailis, A.L. Roytburd, V. Vaithyanathan, D.G. Schlom, T. Zhao, R. Ramesh, *Effect of 90° domain movement on the piezoelectric response of patterned  $PbZr_{0.2}Ti_{0.8}O_3/SrTiO_3/Si$  heterostructures*, Appl. Phys. Lett. 87 072907, 2005
- [1] T. Takenaka, *Piezoelectric Properties of Some Lead-Free Ferroelectric Ceramics*, Ferroelectrics, 230, 87-98, 1999
- [1] G. A. Smolenski, V. A. Isupov, A. I. Agranovskaya, N. N. Krainik, *New ferroelectrics of complex composition*, Sov. Phys. Solid State 2 2651 196, 1961
- [1] E. Aksel, J. L. Jones, *Advances in Lead-free piezoelectric materials for sensors and actuators (Review)*, Sensors, 10, 1935, 2010
- [1] T. Takenaka, K. Maruyama, K. Sakata,  *$(Bi_{1/2}Na_{1/2})TiO_3-BaTiO_3$  system for lead-free piezoelectric ceramics*, Jpn. J. Appl. Phys., 30, 2236, 1991
- [1] A. Purice, G. Dinescu, N. Scarisoreanu, P. Verardi, F. Craciun, C. Galassi, M. Dinescu, *Ferroelectric thin films obtained by pulsed laser deposition*, Journal of the European Ceramic Society 26, 2937, 2006
- [1] M. Dinescu, F. Craciun, N. Scarisoreanu, P. Verardi, A. Moldovan, A. Purice, A. Sanson, C. Galassi, *Ferroelectric  $(Na_{1/2}Bi_{1/2})TiO_3-BaTiO_3$  thin films obtained by pulsed laser deposition*, J. Phys. IV France 128, 77-80, 2005

[1] S. Su, R. Zuo, *Fabrication and electrical properties of  $0.94\text{Na}_{0.5}\text{Bi}_{0.5}\text{TiO}_3\text{-}0.06\text{BaTiO}_3$  textured ceramics by RTGG method using micrometer sized  $\text{BaTiO}_3$  plate-like templates*, Journal of Alloys and Compounds, Volume 525, Pages 133–136, 2012

[1] N. D. Scarisoreanu, F. Craciun, A. Chis, R. Birjega. A. Moldovan, C. Galassi, M. Dinescu, *Lead-free ferroelectric thin films obtained by pulsed laser deposition*, Applied Physics A: Materials Science and Processing, 101 , 747, 2010

[1] G.Picht, J. Töpfer, E.Henning, *Structural properties of  $(\text{Bi}_{0.5}\text{Na}_{0.5})_{1-x}\text{Ba}_x\text{TiO}_3$  lead-free piezoelectric ceramics*, J. Eur. Ceram. Soc, 30, 3445, 2010

[1]T.Takenaka, *Piezoelectric Properties of Some Lead-Free Ferroelectric Ceramics*, Ferroelectrics, 230, 87-98, 1999

---